EFDA-JET-CP(06)04-18

I. Nunes, P. de Vries, P. Lomas and JET-EFDA contributors

Optimization of the JET Beryllium Tile Profile for Power Handling

Optimization of the JET Beryllium Tile Profile for Power Handling

I. Nunes[1], P. de Vries[2], P. Lomas[2] and JET-EFDA contributors*

[1]Associação EURATOM-IST CFN/IST, 1049-001 Lisboa, Portugal
[2]EURATOM/UKAEA Fusion Association, Culham Science Centre, Abingdon, OX14 3DB, UK
**See annex of J. Pamela et al, "Overview of JET Results",*
(Proc.20th IAEA Fusion Energy Conference, Vilamoura, Portugal (2004).

Preprint of Paper to be submitted for publication in Proceedings of the
SOFT Conference,
(Warsaw, Poland 11th – 15th September 2006)

ABSTRACT

The primary objective of the JET ITER-like wall project is to install a beryllium main wall and a tungsten divertor. For Beryllium, melting and thermal stress limit the maximum power density which can be tolerated in operation. The tile design has to allow routine plasma operation for ITER relevant scenarios, i.e., $q_{95} \approx [2.3-10]$ with high power input ($P_{in} \leq 30$MW) for pulse lengths of ≈10 s. This paper focuses on the power handling studies of the beryllium tiles for the outer poloidal limiters and ICRH horizontal protections, and the optimization of their design to achieve the operational goal described above.

1. INTRODUCTION

Among the main concerns for ITER operation are the wall lifetime and tritium retention [1][2]. For this reason, although most present devices have a full carbon wall, ITER will have Be for the main wall and tungsten (W) for the divertor with CFC only on the target. It is expected that this choice will change the carbon erosion and redeposition behaviour and most probably relax the T-retention problem compared to a full carbon device. However, to predict the lifetime and Tritium retention under these conditions a tokamak experiment having an ITER like material composition is needed. At JET, beryllium was used as a plasma facing material in the period between 1990-1995 where several components, amongst them the toroidal belt limiters, were made of Be. An overview of JET operations with Beryllium can be found in Refs. [3][4][5][6]. To answer the critical questions for ITER, the plasma facing components of JET, presently in CFC, are going to be replaced by Be in the main chamber (where possible) and by W in the divertor. The number of limiters, toroidal width and their position remains almost unchanged. The JET tokamak has several poloidal limiters, which define the plasma boundary during limiter operation and protect the RF and LH launchers during X-point high power operations. Presently, these are designed to handle power for a single field-line helicity, only the inner wall guard limiter allows both helicities. The poloidal limiters are not spread toroidally equidistantly over the machine. Hence the connection length varies from limiter to limiter, therefore influencing the scrape-off layer length (λ) [7]. Empirically determined values of the scrape-off layer length were found to be in the range λ= 0.4-0.8 cm [3]. Smaller lengths are found at higher plasma current and during H-mode phases. For the calculations of the Be tiles of JET, the values for λ are assumed 1cm for the Low-Field Side (LFS) and 2cm for the High-Field Side (HFS). The precise value is not important, the design must tolerate a range in λ of approximately 2.

The JET limiter Be tile assemblies are to be assembled as a set of slices, held together by a carrier. The tile assemblies are separated by a finite gap (~2–3mm) with its lowest limit defined by the limiter curvature and space for remote handling tools and machine tolerances. The slices are castellated [8] to reduce thermal stresses and eddy currents, but this exposes the toroidally and poloidally facing surfaces, not only from tile to tile but also in the tile itself, to very high power loads. Therefore, ideally, the design would shadow the castellation edges. More seriously, the likely misalignment from slice to slice and/or from tile to tile would increase the exposed area of the edges and cause significant melting.

The melting temperature limit for Be is 1289^{o}C, which corresponds to a energy limit of 6MW/m^2 for 10s (cold vessel). This paper describes the basic concepts for the tiles design in section 2 and in section 3 the influence of the toroidal flux surface curvature on the power density calculations. Section 4 describes in detail the design of the wide poloidal limiters and section 5 that of the horizontal cross beam for the ICRH antenna. Finally, section 6 gives a brief summary of the tile design.

2. Power density for limiters in the scrape-off layer

For a characteristic length of the scrape-off layer λ, and a power loss, P_{loss}, through the Last Closed Flux Surface (LCFS), the power density at a certain distance (z) into the Scrape-Off Layer (SOL) is given by $Q_{SOL} = (P_{loss}/4\pi R\lambda)e^{-z/\lambda}$. The SOL surface is approximated by 2πR (where R is the SOL major radius) and exponential power decay with z is assumed. It is also assumed that power flows in both directions along the flux surfaces. The power density along the field lines can then be evaluated from $Q_{||} = Q_{SOL}/\sin(\zeta)$ where ζ is the field line angle defined by $\tan(\zeta) = B_{POL}/B_{TOR}$ (the ratio of the poloidal to toroidal field components). From these equations we can derive the power density in the poloidally and toroidally facing surface

$$Q_{POL} = \frac{P_{loss}}{4\pi R\lambda}\, e^{-z/\lambda} \quad Q_{TOR} = \frac{P_{loss}}{4\pi R\lambda \tan(\zeta)}\, e^{-z/\lambda} \tag{1}$$

For a surface defined by angles θ and α, to the toroidal and poloidal direction respectively, the glancing angle η(as shown in figure 1), is given by

$$\sin(\eta) = \frac{\tan\alpha\sin\zeta + \tan\theta\cos\zeta}{\sqrt{1 + \tan^2\alpha + \tan^2\theta}} \tag{2}$$

and the power density on the surface for a LCFS aligned with the limiter geometry, is given by

$$Q_{surf} = \frac{P_{loss}}{4\pi R\lambda}\, e^{-z/\lambda}\, \frac{1}{\sin\zeta}\, \frac{\tan\theta\cos\zeta + \tan\alpha\cos\zeta}{\sqrt{1 + \tan^2\alpha + \tan^2\theta}} \tag{3}$$

Where, for the LFS, the SOL major radius R = 4m and λ = 1cm and for the HFS, R = 2m and λ = 2cm.

3. TOROIDAL FLUX SURFACE CURVATURE

The toroidal curvature of the flux surfaces will affect the power density on the tile [7]. By taking this curvature into account (figure 2), the distance from a point on the limiter surface to the LCFS is then given by $r = \pm(R - \sqrt{(R \pm z)^2 + y^2})$ replacing z in the power density equations defined in section 1. The flux surface curvature also changes the angle of impact (θ') of the field line on the limiter surface. By approximating the circular flux surface, this angle is determined as: $z = \mp y^2/2R \rightarrow dz/dy = \tan\theta' = \mp y/R$. The plus sign is for the case of limiters at the LFS and the minus sign for the HFS, as shown in figure 2. The change in the impact angle and SOL depth has opposite effects on the power density as shown in figure 3; at the outer poloidal limiter it yields a decrease of power density, while

the peak power density at the inner tile shifts to the edge of the limiter. The effect is larger at the inner wall because of the smaller radial position of this tile, and hence a larger flux surface curvature.

4. THE POLOIDAL LIMITERS

4.1. TILE SURFACE

For the outer poloidal limiters, a number of different tile shapes have been considered. The design that best satisfies the criteria determined by the adequate power handling and shadowing of exposed edges, can be defined by a polynomial equation $y = c_1x + c_2x^2 + c_4x^4 + c_{10}x^{10}$, where x is the toroidal dimension of the tile and c_1, c_2, c_4 and c_{10} are such, that the power density distribution is constant on the tile surface as shown in figure 4. To allow shadowing from tile to tile the poloidal direction is chamfered by an angle α. The resulting surface is shown in figure 5(a). The symmetry of the tile allows single field-line helicity. This symmetry creates a natural ridge crossing several castellations exposing surfaces to power loads that can be higher than 200MW/m^2, depending on the field line angle, much above the melting limit. The shadowing of these surfaces is possible but it showed to be very complex to machine. Originally, because of eddy currents and thermal stresses [8], each assembly was made by a set of slices (as in figure 5(b)) separated by a gap of 0.6 mm. However, to limit edge exposure in the ridge region, it was decided to build a central block, that includes the ridge and the triangular cuts (this will be discussed later), with 0.35mm grooves. The maximum allowed depth of the exposed toroidally facing surfaces in this block is 40μm. Calculations show that such a value is below the melting limit for a P_{loss} of 10MW for 10s [8], thanks to prompt conduction to the bulk of the material.

4.2. SHADOWING

Between each tile assembly there is a finite gap. This gap exposes part of the poloidally facing surface of each assembly, as shown in figure 6(a), which, for low field line angles gives power loads that would restrict the limiter power handling. Therefore it is necessary to shadow these surfaces. The shadow is determined by the field line angle, the gap width, the toroidal curvature and the chamfer angle. Also the likely misalignment from assembly to assembly has to be taken into account. As shown in figure 6(a), the top of the poloidally facing surface is exposed and closer to the LCFS, which will lead to an increase of the power load on this surface. The shadowing from assembly to assembly, is then obtained by making small triangular cuts on both top and bottom sides of the assembly (as shown in figure 6(b)) creating two small ridges which will allow the shadowing of the poloidally facing surface in the region of the highest power density even in case of misalignment. Because of the specific design of the Beryllium tiles assemblies, the toroidally and poloidally facing surfaces in the grooves, outside the central block, will also be exposed. The shadowing of the toroidally facing surfaces is obtained by increasing the height of slice 1 (figure 7) relative to slice 2, by the difference d, given by the tile curvature, plus a tolerance, t, in this case with a maximum of 200μm. As for the poloidally facing surfaces it was decided not to shadow them, by assuming that the groove width is smaller than

the ion Larmor radius (ρ_L = 0.592μm for T_{sep} = 100eV, B_T = 3.45T) preventing in this way the penetration of the field lines into the grooves. For T_{sep} lower than 40eV, ($\rho_L \leq$ 0.35μm), the power density on the poloidally facing surface is determined by the 3D field line penetration on the exposed edge, which depends on the chamfer angle (α) and the gap between grooves (0.35mm). Another consequence of a castellated design is that field line angles can penetrate through the assembly to assembly gap and hit the toroidally facing surfaces created by the groove in between slices (figure 8(a)). The power density in these surfaces is very high, even for distances quite far from the LCFS. An example of the power decay with distance to LCFS for both the toroidally and poloidally facing surfaces for the wide poloidal limiter and a field line angle of 5^o is shown in figure 9. A small chamfer on the slices side is enough to shadow these toroidally facing surfaces, as shown schematically in figure 8(b).

4.3. POWER HANDLING

In this section the study of the power handling for the wide poloidal limiter is presented. The minimum distance between the plasma and the limiter (z or radial outer gap, ROG), necessary to keep the maximum power on the tile surface of 6 MW/m^2 is determined by the equation below, where α is the chamfer angle and θ is the angle of the flux surface with the tile surface where the power load is maximum.

$$z = -\lambda ln\left(\frac{Q_{max}}{Q_0}\ e^{-z/\lambda}\ \frac{\sin\zeta\sqrt{1+\tan^2\alpha+\tan^2\theta}}{\cos\zeta\tan\theta+\sin\zeta\tan\alpha}\right) \quad (4)$$

Figure 10 shows the minimum distance allowed between the plasma and the limiter as a function of input power for several field line angles (q_{95}) for a maximum power density on the tile surface of 6MW/m^2. For example a plasma with q_{95} = 2.7 could allow a maximum input power of approximately 15 MW, while for a high q_{95} plasma (11.4) the maximum input power would be ≈ 4MW. These values are taken for a LCFS that sits at the tile surface. Plasma with ROG higher than 2.5cm, and high q_{95} (ζ = 5 degrees) will allow P_{IN} = 30MW for 10s without reaching the tile power density limit.

5. ICRH CROSS BEAM

5.1. TILE SURFACE

All the poloidal limiters have the same design concept with some adjustments to accommodate constraints specific to each limiter. However, the protection of the ICRH antenna also includes two horizontal cross beams 5mm recessed from the wide poloidal limiter. In this case, the gaps between tiles will expose the toroidally facing surface. With 6MW/m^2 on the wide poloidal limiters, the power density on this surface, 5mm into the SOL, when exposed is 138MW/m^2. Therefore, the design of these tiles has to be such that the toroidally facing surfaces are almost totally shadowed or chamfered in order to reduce their power density at these surfaces. The design used for the poloidal limiters does not allow good shadowing of these surfaces. The decrease of the power load on the toroidally facing surfaces is achieved by defining the tile surface as a semicircle and by rotating it

by an angle δ as shown on figure 11. In this case, the surfaces of the slices that are exposed to the field lines are at low angle, and therefore, "see" a much smaller power density (in this case Q_{surf}). The tolerance to misalignment is handled by the triangular cuts. Due to machining complexity, the assembly is made of separate slices with the size of one castellation with a width of 14mm and height of 50mm, separated by a 3 or 3.375mm gap and a tolerance to radial misalignment of 0.5mm.

5.2. SHADOWING

The rotation angle (δ) also defines the shadow cast from one slice on the adjacent slice. Figure 11 shows two slices where the second slice is misaligned by 0.5mm for the case where δ = 10∞ and a field line angle (ζ) of 10^o where the red envelope shows the exposed tile surface. However, because the power density on the toroidally facing surface is very high, it is important to know how far into the SOL is the shadowing effective. By varying δ is possible to vary the distance into the SOL to which the toroidally facing surface is exposed. For $\delta = 10^o$, there is exposure of this surface for distances into the SOL higher than 18 mm, where the power density is 20MW/m^2. For $\delta = 20^o$, the toroidally facing surface starts to be exposed at distances into the SOL higher than 27mm. In this case the power density is 8.5MW/m^2. For both cases the shadow in the surface is good and δ does not play an important role here. However, Q_{surf} depends critically on the rotation angle.

5.3. POWER HANDLING

To assess the power handling for this type of tile, the worst case is taken into account, i.e., small field line angles, $\zeta = 5^o$ (q_{95}~11.4). Figure 12 shows the surface power density at the toroidal location of maximum Q_{surf} for $\zeta = 5^o$ and $\delta = 10^o$. The maximum power density at the tile surface, in this case, is defined by the triangular cuts. Here, Q_{surf_cuts} is 27.6MW/m^2 while at the tile surface Q_{surf} is ≈ 20MW/m^2.

For shadowing, the higher the rotation angle (δ), the more efficient is the shadowing of the toroidally facing surface. However, it is worse in terms of power handling; increasing δ from 10^o to 20^o increases Q_{surf} from 20 to 30 MW/m^2. Based on these studies, and the fact that there are different tiles and gaps sizes, the design to be installed has a δ of 14 degrees with the triangular cuts determined in order to fulfil the requirements for shadowing, tolerance to misalignment and power handling (for z ≥ 3.7cm).

SUMMARY

The complexity of the design for the Be tiles of all the limiters at JET is increased by the fact that, differently from the CFC tile design, each tile is an assembly of castellated slices, exposing the toroidally and poloidally facing surfaces. In this paper only the design for two sets of tiles has been described. For this design, the basic concepts to define the tile shape are described. The tile design has to take into account three major constraints: to be able to handle 6MW/m^2, the power handling of the tile has to be limited by the tile surface therefore, all toroidally and poloidally facing surfaces with power densities higher than the power density of the surface have to be shadowed and, finally, it has to cope

with the tolerances to misalignment from slice to slice and tile to tile. The major difficulty is due to the castellations. The power density on the exposed toroidally and poloidally facing surfaces is such that if not shadowed, the tiles will melt. The complexity of the shadowing of these surfaces is simplified by achieving a compromise between structural limits and machining, where an assembly is made of a few castellated blocks and not as a set of slices.

Although the structural support for the limiters was not originally designed for castellated Be tiles but for single piece solid tiles, it has been shown in this paper that it is possible to achieve such a design that has similar power handling as to the CFC tiles and obeys the constraints imposed by the Be material. In principle, these designs are ready for manufacture, but an independent check with field line following of representative plasma equilibria will be performed.

Acknowledgments

This work has been carried out in the frame of the Contract of Association between the European Atomic Energy Community and Instituto Superior Técnico (IST) and of the Contract of Associated Laboratory between Fundação para a Ciência e Tecnologia (FCT) and IST. The content of the publication is the sole responsibility of the authors and it does not necessarily represent the views of the Commission of the European Union or FCT or their services.

References

[1]. Federici G. *et al*, "Wall and edge research at JET – 2008 and beyond" Nucl. Fusion, **41**, 12R (2001) 1967

[2]. Philipps V., Roth J., Loarte A., 30th EPS, St. Petersburg, July 2003, "Key Issues in Plasma-Wall Interactions for ITER: A European Approach"

[3]. E. Deksnis, *et al.*, Fusion Engineering and Design **37** (1997) 515

[4]. Loarte A, *et al.*, 'A new look at JET operation with Be as plasma facing material', J. Nuc. Mat. **337-339** (2005) 816-820

[5]. E. Deksnis, *et al.*, 'Damage to JET beryllium tiles', J. Nucl. Mat. **176-177** (1990) 583

[6]. P.R. Thomas, *et al.*, 'Results of JET operation with beryllium', J Nucl. Mat. **176-177** (1990) 3

[7]. E. Deksnis, 'The JET belt limiter tiles', JET-R(88)19

[8]. Thompson, V., this conference

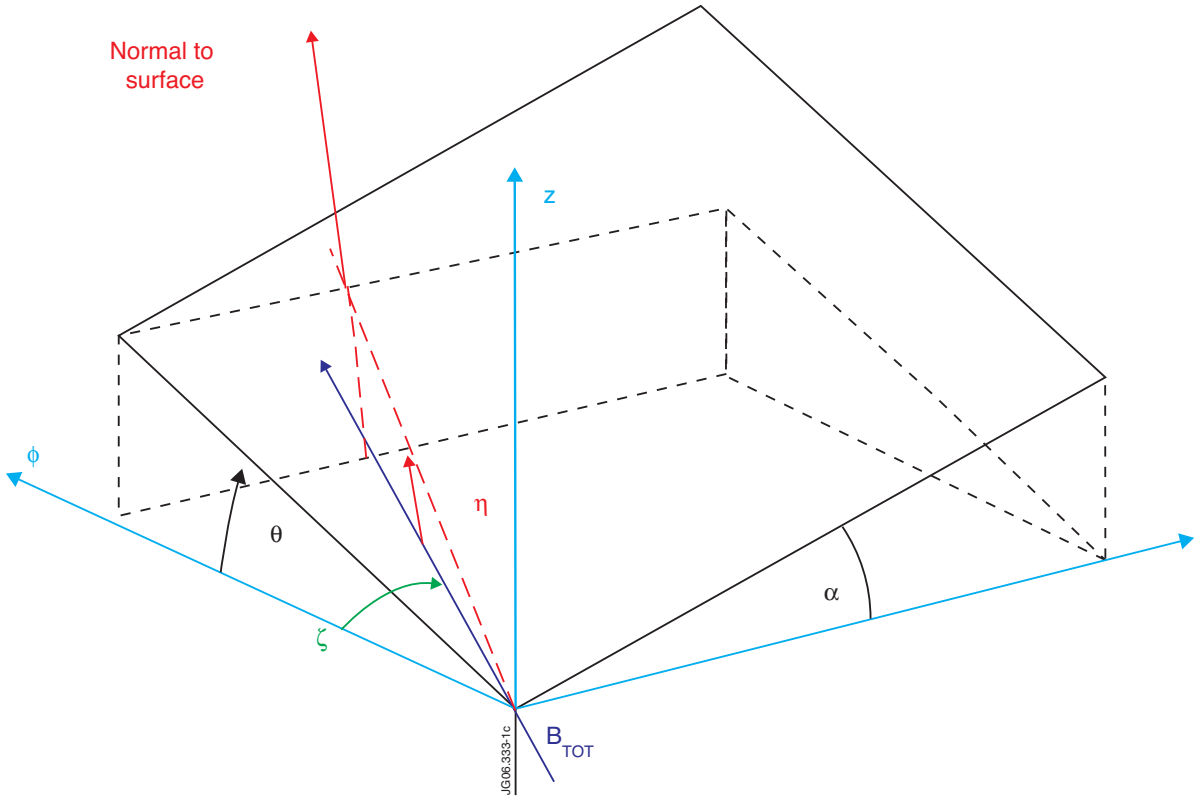

Figure 1: The total magnetic field (B) is in the toroidal-poloidal plane ϕ–φ and at an angle ζ to the toroidal direction. The plane of the surface is defined by the angles θ and α relative to the ϕ–φ plane.

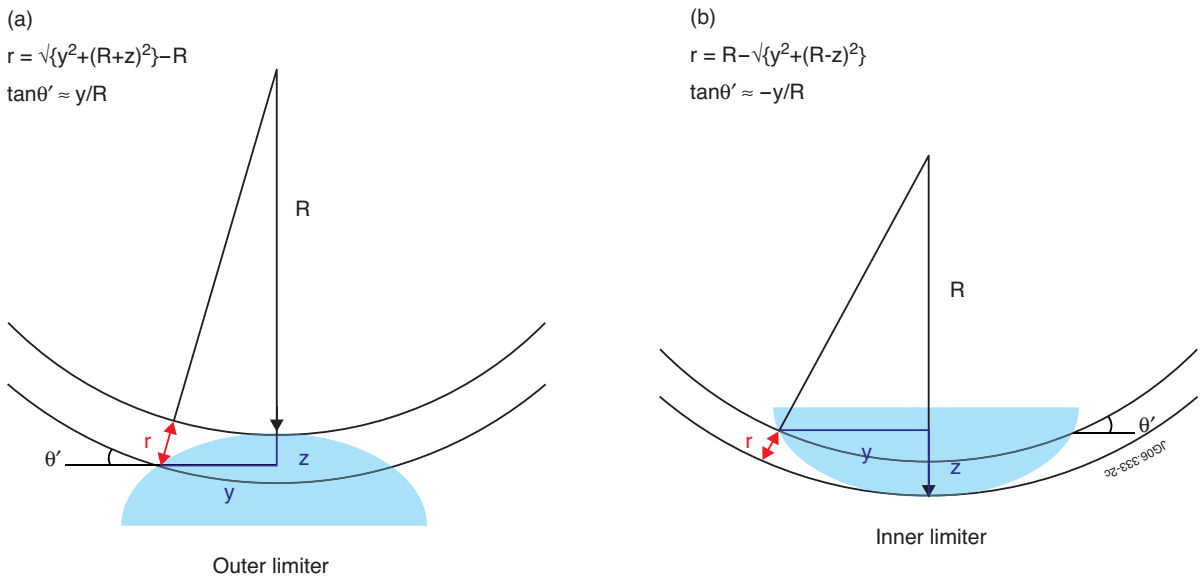

Figure 2: The curvature of the LCFS with respect to the tile curvature may affect the power handling of a tile. This effect differs between a) an outer poloidal limiter and b) one on the inside, like the inner wall guard limiter

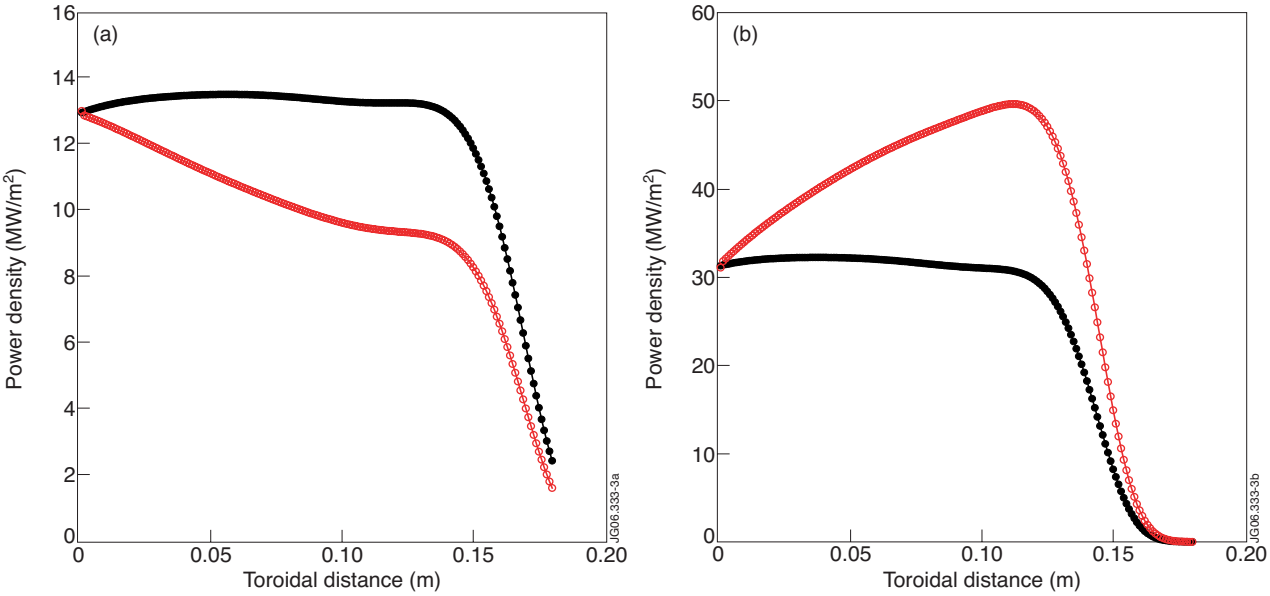

Figure 3: Power density distribution (a) LFS and (b) HFS, for an optimized tile surface curvature without the correction of the flux surface curvature (blue curves) and including the effect due the flux surface curvature (red curves).

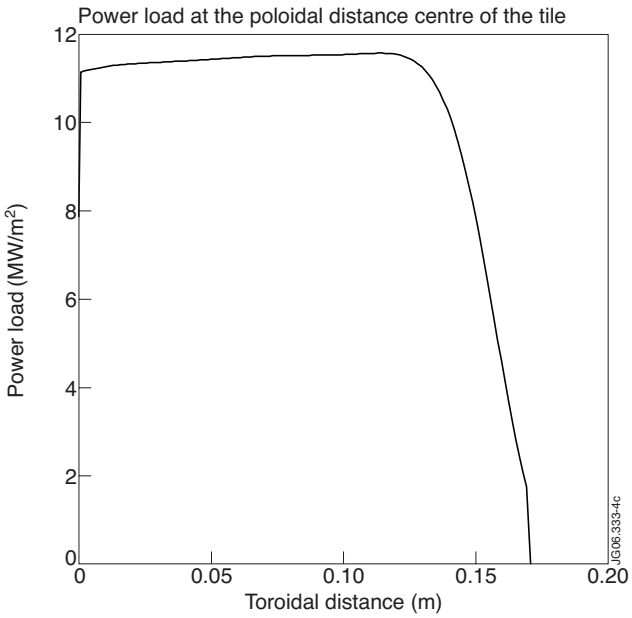

Figure 4: Example of the power density distribution at the tile surface for the wide poloidal limiter

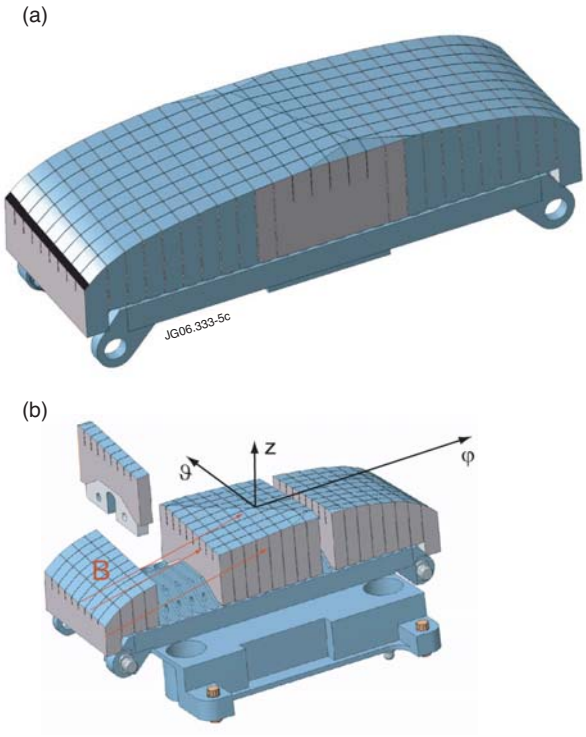

Figure 5:(a) Tile surface for the wide poloidal limiter (b) example of a tile assembly, with the coordinate axis and, schematic incidence of the field lines (B) on the various tile surfaces.

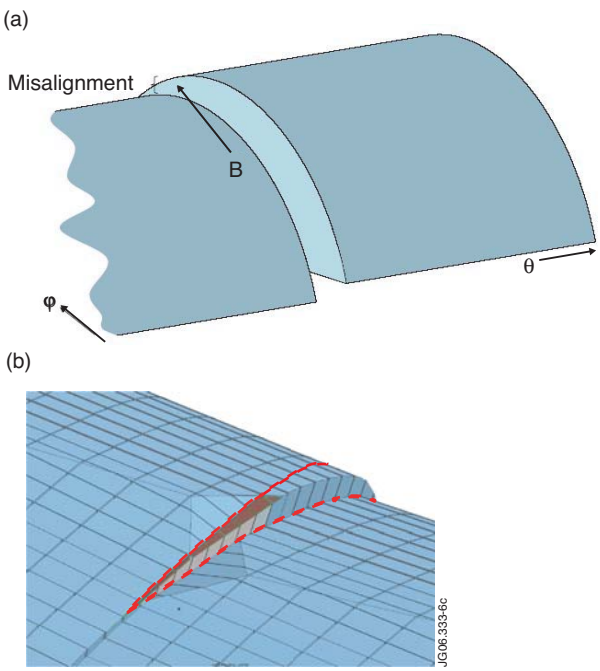

Figure 6: (a) gap and misalignment from assembly to assembly. (b) Lateral cuts to shadow poloidally facing surfaces exposed due to the gap from assembly to assembly (red line).

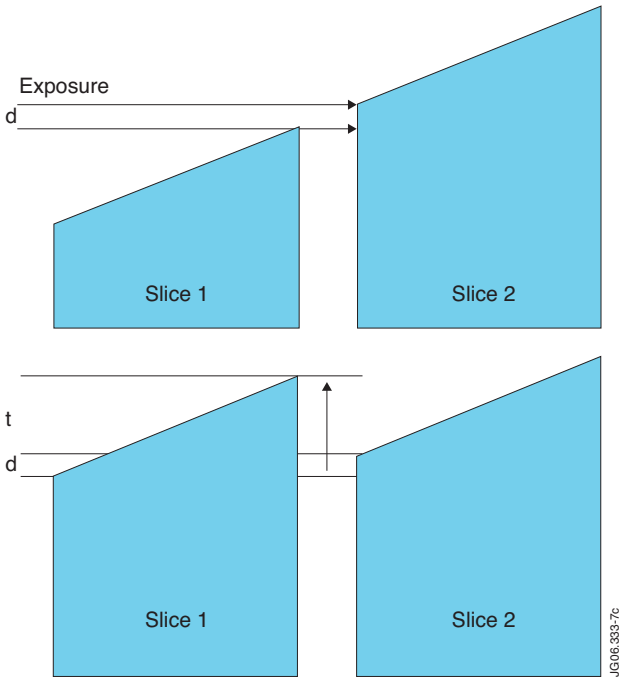

Figure 7: Shadowing of the toroidally facing surfaces from slice to slice

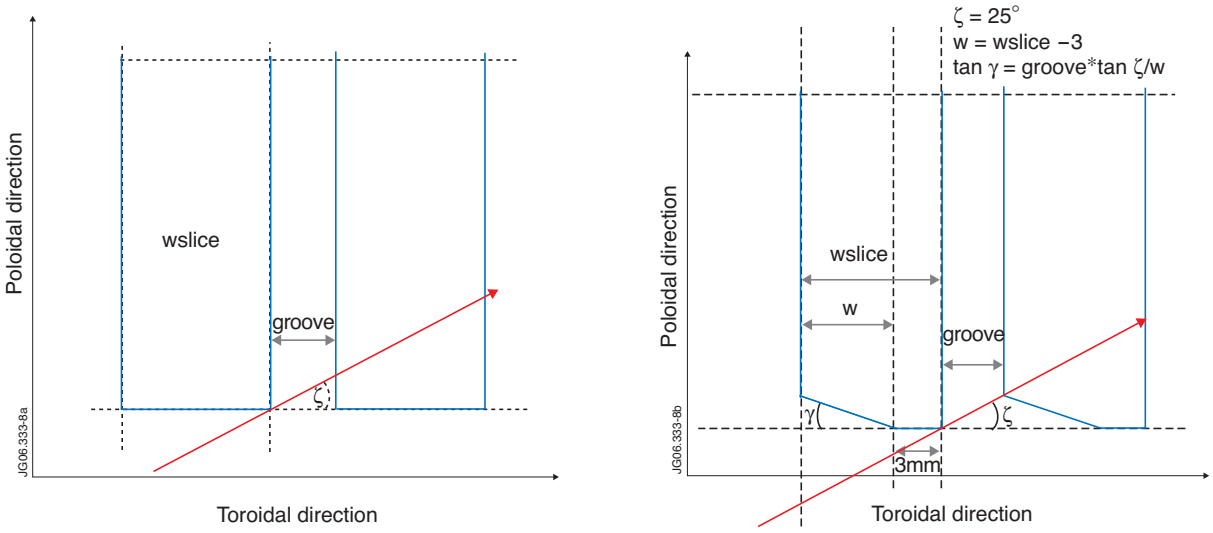

Figure 8: (a) Exposure of the toroidally facing surfaces due to the gap from slice to slice and (b) determination of the minimum chamfer angle to avoid the exposure of these surfaces.

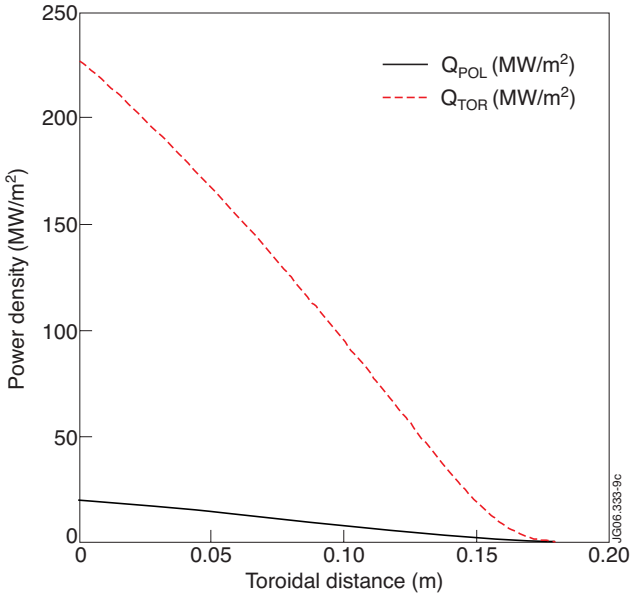

Figure 9: Power density for the toroidally (red) and poloidally (blue) facing surfaces.

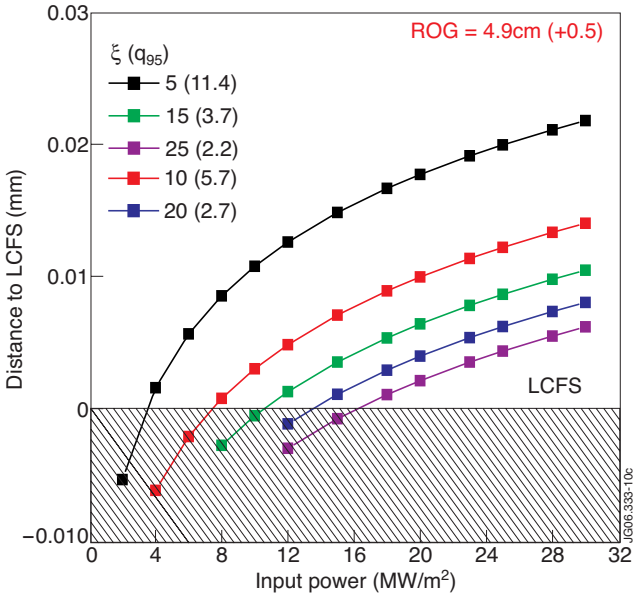

Figure 10: Distance needed between the LCFS and the tile surface for a limit of the power load on the surface of 6MW/m^2. For example, for an input power of 20MW the tile has to be ~2 cm away from the LCFS for ζ = 5 degrees (q_{95} = 11.4)

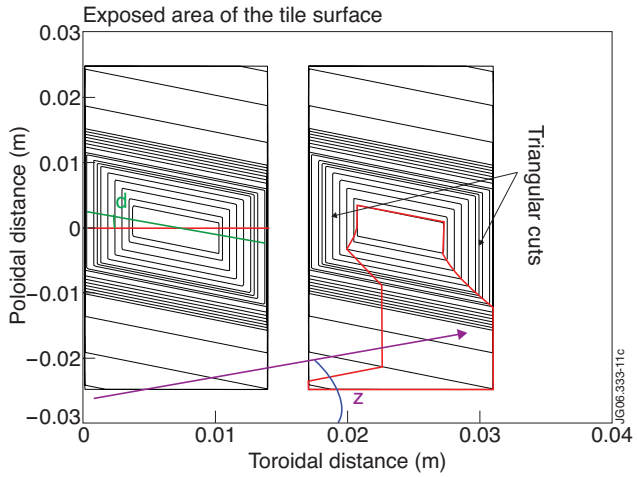

Figure 11: Contour plots of the shaped slices for a rotation angle (δ) of 10^o and ζ = 10^o and a misalignment of 0.5mm. Also shown are the triangular cuts on the sides of the tiles to deal with the tile to tile shadowing and misalignment. The red envelope shows the exposed area of the tile surface.

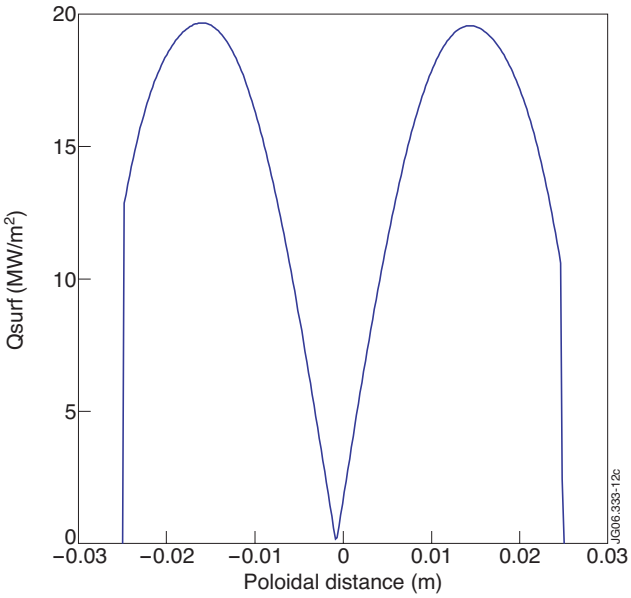

Figure 12: Q_{surf} at the toroidal location where Q_{surf} is maximum.